Published in final edited form as:
J Biomed Mater Res A. 2013 January ; 101(1): 203–212. doi:10.1002/jbm.a.34309.

Correlating macrophage morphology and cytokine production resulting from biomaterial contact

Hyun-Su Lee[1,2], **Stanley J. Stachelek**[4], **Nancy Tomczyk**[1], **Matthew J. Finley**[4], **Russell J. Composto**[2,3], and **David M. Eckmann**[1,3]

[1]Department of Anesthesiology and Critical Care, University of Pennsylvania, Philadelphia, PA, USA

[2]Department of Materials Science and Engineering, University of Pennsylvania, Philadelphia, PA, USA

[3]Institute for Medicine and Engineering, University of Pennsylvania, Philadelphia, PA, USA

[4]Division of Cardiology, Department of Pediatrics, The Children's Hospital of Philadelphia, Philadelphia, PA, USA

Abstract

The morphological and inflammatory responses of adherent macrophages are correlated to evaluate the biocompatibility of surfaces. Monocyte derived macrophage, THP-1, and THP-1 cells expressing GFP-actin chimeric protein were seeded onto glass, polyurethane (PU), and glass surface modified with quaternary ammonium salt functionalized chitosan (CH-Q) and hyaluronic acid (HA). Using confocal microscopy, the surface area, volume and 3-D shape factor of adherent macrophages was quantified. For comparison, functional consequences of cell-surface interactions that activate macrophages and thereby elicit secretion of a pro-inflammatory cytokine were evaluated. Using an enzyme linked immune sorbent assay, tumor necrosis factor-alpha (TNF-α) was measured. On glass, macrophages exhibited mainly an amoeboid shape, exhibited the largest surface area, volume, and 3-D shape factor and produced the most TNF-α. On PU, macrophages displayed mainly a hemispherical shape, exhibited an intermediate volume, surface area and 3-D shape factor, and produced moderate TNF-α. In contrast, on CH-Q and HA surfaces, macrophages were spherical, exhibited the smallest volume, surface area, and 3-D shape factor, and produced the least TNF-α. These studies begin to validate the use of GFP-actin modified MDM as a novel tool to correlate cell morphology with inflammatory cell response.

Keywords

Macrophage; biocompatibility; cell morphology; biomaterials; inflammation

INTRODUCTION

The biocompatibility of synthetic and natural materials is of great interest, in part, because of the new materials developed to replace body parts (e.g., tissue and organs) or function while in direct contact with living tissue. Despite advances in materials design, biomaterials do not behave like native biological structures and incite blood clotting and tissue inflammation, and are susceptible to infection.[1–5] Thus, facile and accurate methods for

*Correspondence should be addressed to: David M. Eckmann, Ph.D., M.D., 331 John Morgan Building, 3620 Hamilton Walk, Philadelphia, PA 19104-6802, USA, Tel.: +1 215 349 5348; fax: +1 215 349 5078, David.Eckmann@uphs.upenn.edu (D.M. Eckmann).

screening and evaluating the biocompatibility of biomaterials are required. To avoid human risk and minimize animal experimentation with *in vivo* testing, *in vitro* methods such as cell and blood compatibility have been developed.[6] Because of their characteristic response to foreign materials, macrophages are attractive cells for evaluating the biocompatibility of implants and medical devices.[7–10]

Macrophages, derived from monocytes, play a key role in the phagocytosis of cellular debris and pathogens, as well as in the foreign body responses resulting from organ transplantation, biomaterial implantation, and microbe infection. Macrophages actively respond to many implants *in vivo*, including metals, ceramics, and polymers.[11–16] In general, adherent macrophages on biomaterials react by attempting to phagocytose the foreign body. Subsequent pro-inflammatory cytokine secretion, such as release of tumor necrosis factor (TNF-α), interleukins (IL-1, IL-6), and chemokines (IL-8), directs the inflammatory and wound healing response to the biomaterial. Macrophages have been used to interrogate biomaterials by investigating their activity and secretion of pro-inflammatory cytokines.[17–23]

In spite of the fact that a correlation between cell morphology and surface properties has been well established, few methodologies exist that allow for the dynamic analysis of the inflammatory response in living cells. For example, adherent macrophages can exhibit an amoeboid, elongated spindle-like, or round shape depending on their lamellipodial extensions.[18,24] Thus, spreading behavior is an indicator of cell morphological response to surface type and surface interactions. To quantify this response, cell attachment area has been measured using scanning electron microscopy (SEM), laser scanning confocal microscopy (LSCM), fluorescent microcopy, and bright field microscopy.[8,18,22,25–28]

Although inflammatory cytokine-associated response to biomaterials is well known, the interrelationship between the morphological responses of macrophages with secretory function has received little attention. In these studies, we begin to validate the use of an actin-GFP expressing monocyte derived macrophage (MDM) cell line as a viable imaging tool to assess, in living cells, how cell morphology relates to the inflammatory status. Here, we hypothesize that both macrophage morphology and secretory response reflect the biocompatibility of the surface and correlate with each other. Four complementary surfaces are investigated. Glass is our control surface. Polyurethane (PU) is a common biomaterial used in medical applications and is moderately biocompatible.[25,28,29] A polymeric monolayer coating of chitosan modified with quaternary ammonium salts (CH-Q) is grafted to silicon oxide (glass). CH-Q is highly positively charged across a wide pH range, antibacterial and strongly swells at physiological conditions.[30,31] To complement surfaces prepared with the polycationic polymer, CH-Q, hyaluronic acid (HA), a negatively charged polymer, is grafted to silicon oxide (glass).[24] Thus, macrophage morphology and secretory response can be compared on surfaces having widely different characteristics (e.g. charge). Cell morphology is used to interpret the response of adherent cells on each surface by measuring the cell-surface interfacial area, cell volume, and 3D shape factor. The secretion of the pro-inflammatory cytokine TNF-α, a classical *in-vitro* evaluation of biocompatibility,[17,19–23] is monitored. Our studies demonstrate that adherent macrophage morphology is integrally related to the cellular activation state resulting in cytokine secretion and that this response is decidedly surface type dependent. Whereas unmodified glass is known to stimulate significant biological responses, our studies show that PU provokes a greater biological response than glass surfaces functionalized with CH-Q or HA, which are the surfaces that elicit the minimum biological response.

EXPERIMENTAL

Materials

Chitosan Chitoclear® Cg-10 (Mw = 60 kDa and degree of deacetylation: 87%) was received from Primex ehf., Iceland. Polyurethane (Nalgene 280 PUR Tubing; using a 1,4-butanediol soft segment and 4-4′-methylene diphenyl diisocyanate (MDI) as the hard segment) and hyaluronic acid potassium salt from human umbilical cord (Mw = 750 kDa, #H1504) were purchased from Fisher Scientific and Sigma-Aldrich Co., respectively. 80 wt % aqueous solution of [(2-(acryloyloxy)ethyl]trimethyl ammonium chloride (AETMAC), 3-Glycidoxypropyl-trimethoxysilane (GPTMS, ≥98%), 3-aminopropyltriethoxysilane (APTES, ≥98), tetrahydrofuran (for HPLC, ≥99.9%) and anhydrous toluene (99.8%) were purchased from the Aldrich Chemical Co. USA. Sodium cyanoborohydride ($NaBH_3CN$), and HEPES were purchased from Sigma-Aldrich Co. and Fisher Scientific. 1-Ethyl-3-(3-dimethylaminopropyl) carbodiimide hydrochloride (EDC) and sulfo-NHS were purchased from Thermo and Fisher Scientific, respectively. Ultrapure water (Millipore Direct-Q, 18 MΩ cm resistivity) was used for surface preparation.

Surface preparation

Glass Petri dishes and silicon wafers were cleaned using piranha solution (3:1 (v/v), H_2SO_4/30%H_2O_2) to create silanol groups that react with GPTMS and APTES, respectively. Using clean silicon oxide surfaces, GPTMS and APTES reactions were carried out immediately. The thickness and water contact angle of GPTMS and APTES grafted to surfaces were verified by ellipsometry (Rudolph AutoEL II) and contact angle goniometry, respectively. To graft, hyaluronic acid, HA, to surfaces, EDC-mediated condensation with N-hydroxysuccinimide was used.[24,32–34] Specifically, the APTES (amine) glass surface was immersed in a solution containing hyaluronic acid (2 mg/mL), EDC (38.2 mg/mL), sulfo-NHS (10.8 mg/mL) and HEPES (2.3 mg/mL) for one day at room temperature. The HA grafted surface was washed with water and dried using nitrogen. Using a known method,[30,31] chitosan with quaternary ammonium salts, CH-Q, was grafted to epoxide-derivatized (GPTMS) glass by immersing the GPTMS surface in 2wt % aqueous solution (10 mL) of CH-Q (pH 7.8) at 60 °C for ~12 hr. The surface was rinsed with water to remove residual impurities. Polyurethane (PU) coated surfaces were prepared by spin coating (2000 rpm) a 3 wt% solution of PU in THF onto glass, followed by drying in vacuum (~40 millitorr) for one day (i.e. residual THF in thin PU layer (100 nm) is removed under this condition because its low glass temperature (T_g = ~40 °C)[35] leads polymer chains to diffuse at room temperature). The thickness and contact angle of HA and CH-Q modified surfaces and PU spin-coated surfaces were subsequently verified by ellipsometer and contact angle goniometer measurements for the same solution spun-cast on a silicon wafer, respectively. Contact angles of HA, CH-Q and PU layers were 21 ± 5°, ~0°, and 70 ± 2°, respectively. Before using these samples for cell culturing, the layers were immersed in autoclaved DI water for several days with shaking at 40 rpm.

Actin-GFP

The plasmid pAcGFP1-Actin, encoding green fluorescent protein (GFP) and cytoplasmic β-actin, was purchased from Clontech (Mountain View, CA). Enzyme restriction digests were performed to insert the GFP-Actin fusion gene into a custom modified self-inactivating, replication incompetent HIV-1 based viral vector.[36] The GFP-Actin fusion gene was inserted immediately downstream of the human CMV immediate early promoter. Viral vectors were generated in 293T cells and the supernatant was collected and processed as reported previously.[37]

Macrophage cell culture

The Human monocytes, (THP-1 obtained from ATCC and GFP-actin transduced THP-1), were cultured in RPMI medium (Cell Culture Technologies, VA), supplemented with 10% fetal bovine serum, 0.05 mM 2-mercaptoethanol, 200 mM L-Glutamine, and 1% Penicillin Streptomycin. As shown in Figure 1, both monocytes were differentiated using 0.2 μM phorbol 12-myristate 13-acetate (PMA) and seeded on sample surfaces in the same cell culture condition, respectively. Both of these cell culture lines were maintained in a 37 °C incubator with 5% CO_2 and under a humidified atmosphere. Unless stated otherwise, experiments were conducted at a cellular concentration of 1.5×10^5 cell/mL.

Transduction of THP-1 cells

The human MDM cell line, THP-1, was grown in complete growth medium, supplemented with 8μg/ml of polybrene, in the presence of the above described GFP-Actin expressing lentiviral vector (MOI = 10) or a GFP expressing lentiviral vector.[36] Fluorescence microscopy, using the appropriate filter set, was used to confirm the expression of both GFP and Actin-GFP. For experimental analysis, GFP expressing THP-1 cells (THP-1GFP) or GFP-Actin expressing THP-1 cells (THP-$1^{GFP\text{-}Actin}$), were transformed with the addition of 0.2 μM PMA to the media for one week prior to analysis as detailed below.

Western blot analysis and immunoprecipitation studies

Cultured THP-1^{GFP}, or THP-$1^{GFP\text{-}Actin}$, cells were processed for Western blot analysis as previously described.[38] Where indicated, an immunoprecipitation was performed as previously described.[38] Briefly, cellular lysates were spun down at 10,000 g for 10 min, and the collected supernatant was first incubated with 5 μg of anti-GFP antibody (as above). The lysate proteins and immunoprecipited proteins were resolved on a 4–15% gradient sodium dodecylsulfate-polyacrylamide electrophoresis gel using the method described by Laemmli.[39] Immunoblotting for the presence of GFP using a rabbit derived anti-GFP antibody (Abcam, Cambridge, MA) at the manufacturer's recommended dilutions in 10 mM pH 7.5 Tris-HCl, 100 mM NaCl, and 0.1 % Tween 20 (TTBS) with 5% non-fat milk. In similar fashion, the immunoprecipitated Actin-GFP complex was processed to detect the presence of Fascin with a goat anti-human Fascin (Santa Cruz Biologics) antibody at the manufacturer's recommended dilutions. The respective immune complexes were detected with the species-appropriate, horseradish peroxidase-conjugated secondary antibodies in recommended dilutions in TTBS with 5% non-fat milk and were visualized with an enhanced chemiluminescence detection system on X-ray films.

DHR-123 assay

Reactive oxygen species (ROS) expression was determined as described previously using a dihyrdorhodamine-123 (DHR-123) detection assay as described previously.[40] Briefly THP-$1^{GFP\text{-}Actin}$ cells or non-expressing THP-1 control cells were stimulated with PMA. After 1 week, attached differentiated THP-1 cells were trypsinized, seeded (10^5 cells/well), and allowed to spread onto the bottom of 96-well plates. Cells were incubated in serum-free media supplemented with 5 mM DHR-123 for two hr at 37 °C and then washed three times with PBS. Where shown, cells were incubated with 10^{-5} M Pargyline for two hours, and then 10 mM of DMNQ was added to the medium. After 2 hr, ROS levels were determined by monitoring the fluorescence of rhodamine generated by the oxidation of DHR-123. Fluorescence was measured at 500 nm (excitation) and 536 nm (emission) using a Spectramax Gemini series spectrofluorometer (Molecular Devices, Sunnyvale CA). Background fluorescence was subtracted from all readings and data were expressed as arbitrary fluorescent units (AFUs).

Cytokine measurement

As described in Figure 1, after three days in culture, TNF-α cytokines were measured for both non-adherent and adherent THP-1 cells, differentiated using 0.2 μM PMA. Fresh RPMI medium was used to rinse these plates and as well as only the adherent cells (c.f., Figure 1). After an additional three days of culturing only adherent cells, the medium was collected to measure TNF-α using a commercially available (Invitrogen Corp. CA, USA) enzyme-linked immunosorbent assay (ELISA) according to manufacturer's instructions. The TNF-α assay measurement was carried out at 450 nm optical density (OD).

Cell morphology and image analysis

As shown in Figure 1, after three days in culture, non-adherent cells were removed using fresh RPMI medium. 2-D images of both macrophage lines and 3-D images of the GFP-actin macrophages were obtained using a Olympus FluoView FV1000 Confocal Microscope. For this research, at least three experiments were performed using four different surface types and at least three images of each experiment were used for 2-D and 3-D image analysis. To determine adherent cell volume, surface area, and the 3-D shape factor, sequential 2-D images were taken from the top to the bottom of adherent macrophages (slice width = 0.5 μm). In order to compute total cell surface area and cell volume, values of the slice perimeter and area from each successive section were determined using ImageJ software from the National Institutes of Health. The cell volume and cell surface area, including the adherent cell-biomaterial surface interfacial area, were computed using a trapezoidal approximation between sections.[41] The surface area and volume to calculate a 3-D shape factor, φ_{3D},[41] were also determined where:

$$\varphi_{3D} = \frac{(Surface\ Area)^3}{36\pi(Volume)^2}$$

Statistical analysis

All data were expressed as mean ±standard deviation. The Student's t-test (unpaired t-test) was used to evaluate data for significant differences between means. We accepted $P < 0.05$ as an indication that statistically significant differences exist between the means.

RESULTS

Transduction of THP-1 cell with GFP-actin and its characterization

We have successfully developed and characterized a lentiviral vector capable of transducing THP-1 cells with the chimeric protein GFP-actin gene. Figure 2A is a representative Western blot analysis showing immunodetection of GFP from THP-1^{GFP} or THP-1$^{GFP\text{-}actin}$ cell lysates. Lysates from THP-1^{GFP} or THP-1$^{actin\text{-}GFP}$ show only a single immunoreactive band. As expected, the immune-detected band from resolved THP-1^{GFP} lysates was ~30 kDa and is consistent with GFP expression. In contrast the band detected from THP-1$^{GFP\text{-}actin}$ was ~70 kDa, consistent with the presense of actin (40 kDa) and GFP (30 kDa). These results further confirmed expression of the GFP-actin protein. As the generation of ROS by monocyte derived macrophages has been shown by our group and others to contribute to the biodegradation of polyurethane elastomers, experiments were performed to ascertain if ROS production was affected by GFP-actin transfection.[40,42] To that end, ROS levels were determined by monitoring the fluorescence of rhodamine generated by the oxidation of DHR-123. We compared the trends in ROS production between non-transfected and GFP-actin transfected THP-1 cells in the presence of known pharmacological agonists (DMNQ) or antagonists (Pargyline) to ROS production. As shown in Figure 2B, identical

trends in ROS expression are observed between the THP-1 and THP-1$^{GFP\text{-}actin}$ cells. Greater ROS expression was observed in the GFP-actin cells, as a result of GFP fluorescence. Immunoprecipitation studies were conducted to identify actin binding proteins that associated with the chimeric GFP-actin protein. As shown in Figure 2C, the actin binding protein Fascin was coprecipitated with the GFP-actin. These data strongly suggest that GFP-actin and native actin have similar characteristics.

Macrophage adhesion and morphology on surfaces

Figure 3A–D shows representative 2-D images of adherent macrophages (PMA-treated THP-1 cells) on glass, PU, CH-Q and HA surfaces. On glass, macrophages adhered and spread significantly, showing an amoeboid morphology similar to the behavior on polystyrene culture dish (not shown). A minority of adherent macrophages also exhibited a round morphology. On polyurethane (PU) surfaces, the adherent macrophages, which spread moderately, exhibited a round morphology. On CH-Q, the adherent macrophages showed a round morphology, similar to the behavior on HA. The adherent macrophages on both CH-Q and HA also had much lower number density (fewer cells per field) and remained much smaller in their attached and spread shape in comparison to macrophages on glass and PU. In addition, the GFP-actin macrophages (PMA-treated GFP-actin transduced THP-1) on the different surfaces also exhibited a cell density, morphology and spreading behavior that was consistent with that observed for the non-GFP-actin transduced cells. Figure 3E shows the surface density of adherent macrophages following surface rinsing described in Figure 1. For glass and PU the cell densities were similarly high ($2.86 \pm 0.11 \times 10^3$ cell/mm^2, $2.52 \pm 0.30 \times 10^3$ cell/mm^2). By comparison, cell density was significantly lower on CH-Q ($7.1 \pm 2.2 \times 10^2$ cell/mm^2) and a full order of magnitude smaller on HA, on which were bound only $1.95 \pm 0.45 \times 10^2$ cell/mm^2.

3-D Morphology of GFP-actin transduced macrophages on surfaces

After culturing the monocyte-derived macrophages (PMA-treated GFP-actin transduced THP-1 cells) on glass, PU, CH-Q and HA, the adherent cell morphology was analyzed qualitatively using 3-D images constructed from confocal fluorescence microscopy images. Figure 4A–D shows the characteristic morphology of the adherent cells on each surface. The adherent macrophages on glass exhibited distinct lamelliopodial extensions and an amoeboid shape, as shown in Figure 4A. The top panel in Figure 4A also shows the actual extension of the cell boundary beyond the densely illuminated cell interior. This may result from the elongation of membrane-associated actin on the cytoplasmic surface of the membrane adjacent to the surface. Adherent macrophages on the PU surface are hemispherical as shown in Figure 4B. The GFP-actin on the cytoplasmic surface of the attached cell membrane appears to radiate continuously from the cell, although the actual boundary of the adherent cell is not clearly demarcated. In contrast, the adherent cells on CH-Q and HA were both shown to exhibit a more spherical shape, as evident in Figures 4C and 4D. These images show that the cells have a lower interfacial contact area on CH-Q and HA, and lamelliopodial extensions are not well developed.

The values of the cell adhesion area, volume and shape factor on glass, PU, CH-Q and HA are given in Figure 5. Figures 5A–B show that adherent macrophages on glass exhibited the largest total surface area ($4.6 \pm 1.0 \times 10^3$ μm^2) and cell volume ($10.8 \pm 2.9 \times 10^3$ μm^3). On PU, the total cell surface area ($2.6 \pm 0.5 \times 10^3$ μm^2) and cell volume ($5.5 \pm 1.3 \times 10^3$ μm^3) were significantly smaller than for glass, as were the surface area and volume on CH-Q ($1.2 \pm 0.2 \times 10^3$ μm^2 and $2.2 \pm 0.6 \times 10^3$ μm^3, respectively) and HA ($1.2 \pm 0.2 \times 10^3$ μm^2 and $3.6 \pm 1.4 \times 10^3$ μm^3, respectively). The computed values of 3-D shape factor appear in Figure 5C. The value was found to be highest for glass ($\varphi_{3D} = 7.2 \pm 0.9$), and by direct comparison significantly lower on both CH-Q ($\varphi_{3D} = 3.3 \pm 0.7$) and HA ($\varphi_{3D} = 3.5 \pm 1.2$).

In comparison to glass, this parameter was not significantly different for cells on PU (φ_{3D} = 5.0 ± 1.4).

Macrophage TNF-α secretion

For the cell culture after three days that includes both suspended and adherent macrophages (Figure 1), the concentrations of TNF-α secreted from both non-adherent cells and adherent cells on glass, PU, CH-Q, and HA surfaces, were 299.0 ± 45.6 pg/ml, 144.5 ± 3.4 pg/ml, 114.1± 2.2 pg/ml and 165.2 ± 18.5 pg/ml, respectively, as plotted in Figure 6A. The levels of TNF-α secretion by cells exposed to PU, CH-Q, and HA surfaces were all statistically significantly lower than for those cells exposed to glass. TNF-α levels were also significantly lower for CH-Q than for either PU or HA.

At the three day time point for cell culture of solely adherent macrophages (suspended cells removed and fresh media having been instilled, see Figure 1), the measured concentrations of TNF-α secreted by adherent cells on glass, PU, CH-Q, and HA surfaces were 746.6 ± 71.5 pg/ml, 394.9 ± 15.1 pg/ml, 58.0 ± 1.6 pg/ml and 12.7 ± 2.8 pg/ml, respectively, as provided in Figure 6B. To provide a more specific index of cell activation by biomaterial surface contact to elicit secretion of pro-inflammatory cytokines, these TNF-α levels were normalized using the cell adhesion densities reported in Figure 3E. Results appearing in Figure 6C show that TNF-α secretion per adherent cell was highest on glass (6.71 ± 0.11 × 10^{-4} pg/cell). TNF-α secretion was significantly lower for cells adherent to PU (4.74 ± 0.18 × 10^{-4} pg/cell) and CH-Q (2.46 ± 0.07 × 10^{-4} pg/cell) surfaces. The lowest TNF-α levels were detected for cells attached to the HA surface (1.57 ± 0.26 × 10^{-4} pg/cell), and this was statistically significantly less than for any of the other surfaces tested.

DISCUSSION

The primary focus of this research was to study the morphological response of macrophages attached to biomaterials and to determine the interrelationship between morphology and inflammatory cytokine-associated production to evaluate biocompatibility. We investigated the morphological response of adherent macrophages towards a hard inorganic material (i.e., glass), a relatively inert (i.e., polyurethane), and two glass surfaces coated with positively and negatively charged polymer brushes (i.e, CH-Q and HA). In parallel we also studied the functional consequences of adherent cell interactions with these surfaces to activate macrophages and thereby elicit secretion of the pro-inflammatory cytokines, TNF-α.

First, we successfully developed and characterized a lentiviral vector capable of transducing THP-1 cells with the chimeric protein GFP-actin gene. Identical trends in ROS expression observed between the THP-1 and GFP-actin transduced THP-1 cells and the co-precipitation of the actin binding protein Fascin with the GFP-actin demonstrated that the GFP-actin expression has no untoward effect upon normal monocyte derived macrophage function and GFP-actin has similar characteristics as native actin. In this study, PMA-stimulated THP-1 cells and GFP-actin transduced THP-1 cells, similar to the phenotype of human monocyte-derived macrophages,[43–45] were employed. 2-D optical microscopy images and 3-D confocal fluorescence microscopy imaging reconstructions were used to assess cell density, volume, surface area, and spreading.

The morphological responses of monocyte-differentiated macrophages (PMA-stimulated THP-1) showed surface-dependent cell morphologies and population densities. Adherent macrophages on glass demonstrated primarily amoeboid and partially round morphologies, as has been reported.[24] In contrast, adherent macrophages spread moderately and showed mainly a rounded shape on PU, a common biomaterial with moderate biocompatibility.[25,28,29] The slightly roundish morphology on PU is consistent with what we

have previously reported.[38] As there is growing interest in macrophage response (e.g., inflammatory M1 v. wound healing M2) this would also be a function of the surface on which the macrophage resides. Similarly, the roundish vs. spread morphology is also expected to be a function of the surface. In addition, the rounded shapes on PU agree with findings reported by Anderson et al.,[8] who presented that adherent macrophages showed a rounded shape in monocyte to macrophage development (3 days) among sequential adhesive events of monocytes at implanted biomaterial surface (an Elasthane 80A Polyurethane) from an in vivo cage study. The cell population density was considerably higher on both glass and PU than was found on HA and CH-Q (Figure 3E). Adherent macrophages on HA, a hydrophilic anionic polymer, did not spread and showed a round morphology. Moreover, macrophages attached to HA had the lowest number density of cells. Although the cells attached to CH-Q, a hydrophilic cationic polymer, exhibited a morphology similar to HA, the surface density was larger. Recently, we showed that adherent macrophages on CD47-functionalized surfaces exhibited a rounded morphology and had a surface density similar to the CH-Q and HA-functionalized surfaces.[38] Our results for macrophage adhesion on these surfaces agree with findings reported by Brodbeck et al.,[26,46] who demonstrated that rank order of hydrophilic, anionic, cationic and hydrophobic biomaterial surfaces were associated with increasing quantities of macrophage adhesion. Although the specific molecular mechanism by which macrophages attach onto a surface has not been fully revealed, a lower density of macrophages indicates better biocompatibility of the surface.

To provide further details, confocal fluorescence microscopy was used to produce 3-D images of macrophages attached to the surfaces. The resultant data include cell surface area and volume, and a 3-D shape factor (φ_{3D}) which reflects cell spreading (Figure 5). First, 3-D imaging of adherent macrophages on glass showed a preference for elongation of membrane-associated GFP-actin as well as distinct lamelliopodial extension, with resultant amoeboid morphology. This morphology has been observed by others.[47–49] Of particular interest is that GFP-actin on the cytoplasmic surface of the attached cell membrane on PU surfaces stretches radially outward from the cell center, in contrast to cell behavior on glass. GFP-actin did not exhibit a similar behavior for cells attached to either CH-Q or HA. Recently, we showed that the polymerized state of actin (i.e., actin elongation) in adherent macrophages correlated with the biocompatibility of surfaces.[38] Specifically, macrophages showed a significantly reduced affinity for polymeric surfaces modified with recombinant CD47, a ubiquitously expressed transmembrane protein that reduces the polymerized state of actin through signaling mechanisms mediated by its cognate receptor, Signal Regulatory Protein alpha, or SIRPα.[50] Second, 3-D quantitative analysis of cell morphology indicates that macrophage surface area and volume as well as spreading behavior depend on surface type. In this regard, the morphology of adherent macrophages on PU, CH-Q and HA was distinct from those adherent to glass. Based on the 3-D shape factors, the degree of cell spreading was much lower on CH-Q and HA than on glass. HA and CH-Q are oppositely charged polymers, with the former being negative and the latter having a high positive charge.[24,29,33]. Despite this important difference the morphological responses of adherent macrophages on CH-Q and HA are remarkably similar, namely, similar values of cell surface areas, volumes, and φ_{3D}. These results lead us to believe that CH-Q and HA surfaces by themselves do not induce any dramatic changes in macrophage shape or size in response to surface contact. This is not the case for glass, which strongly stimulates adherent macrophages so that they enlarge and spread (Figure 4A), resulting in large values for the surface area, volume, and 3-D shape factor. As this experimental technique is useful to determine the morphological responses of adherent macrophages on different biomaterials, it can also be applied to other systems for which confocal microscopy is a useful and valid experimental approach since this method is only limited by the imaging system capabilities. For instance, the cells we have prepared could reasonably be used in 3-D matrices (e.g., tissue scaffolds) and other complex geometries. Ultimately, whether or not they could be

imaged depends on the features of the microscopy system. In an application in which toxins are leached, we surmise that cell death may result. This could reasonably be tracked with another fluorescent dye (with good wavelength separation from the GFP we have used) and another channel of laser illumination in a confocal application.

The distinct morphological responses of macrophages resulting from their interaction with the different biomaterial surfaces studied also have correlates in the cell biofunctional/secretory response, as demonstrated by secretion levels of the pro-inflammatory cytokine TNF-α. Our assays of TNF-α levels for suspended plus adherent macrophages (Figure 6A) indicate that glass stimulates the greatest amount of TNF-α production, whereas the CH-Q layer stimulates the least. For suspended plus adherent macrophages exposed to PU, TNF-α levels were similar to that of the HA surfaces. To investigate the bio-functional/secretory response of only the adherent macrophages, the suspended macrophages and PMA are removed, and then the adherent macrophages are cultured in fresh media for an additional three days without PMA (c.f., Figure 1). Thus, TNF-α production after the additional three days of culturing can only be due to the adherent macrophages. On glass and PU, TNF-α secretion increased by a factor of ~2.5 compared to the level exhibited by the suspended plus adherent macrophages on glass and PU (with PMA) after the initial three day period. In contrast, macrophages on CH-Q and HA exhibited a decrease TNF-α secretion compared to the level produced by the suspended plus adherent cells on CH-Q and HA (with PMA) (Figure 6A and 6B). For the adherent macrophages on the four surfaces, the levels of TNF-α secretion are significantly different from each other (Figure 6B). Our assays of TNF-α levels indicate that glass stimulates the greatest amount of TNF-α production, whereas the HA stimulates the least. This behavior, in part, results from the different cell density of macrophages on each surface. To account for this difference, TNF-α secretion level per adherent cell was determined for each surface. Normalized TNF-α secretion levels per adherent macrophage on each surface (Figure 6C) clearly show that HA activates macrophages less and elicits a lower release of TNF-α than do the other surfaces. By rank order high to low, glass, PU, CH-Q, and HA surfaces provoke decreasing levels of TNF-α secretion. Although this cytokine release measurement at a single time point could not be reflective of that entire dynamic of biocompatibility, it can be useful in considering various clinically-relevant conditions such as: very short term (e.g., hours; cardiopulmonary bypass); intermediate term (e.g., days; indwelling vascular catheters); long term (weeks, months; vascular stents or orthopedic implants).

In summary, these studies show both qualitatively and quantitatively that the morphological responses of adherent macrophages are related to their inflammatory cytokine-associated response. Namely, glass, PU, CH-Q, and HA surfaces provoke decreasing levels of TNF-α. Although similar on CH-Q and HA, the morphological response of adherent cells correlate with TNF-secretion; namely, cell spreading is largest on glass, less on PU and least on CH-Q and HA.

CONCLUSIONS

In this study, a GFP-actin expressing macrophage has enabled parallel studies of cell morphology and biofunctional response. To quantify biocompatibility, cell size, shape and associated cytokine secretion were measured. The data clearly demonstrate that the interaction between adherent macrophages and a biomaterial is significantly influenced by surface type. Specifically, the morphological appearance of adherent macrophages and their resultant cell functional activation states resulting in pro-inflammatory cytokine secretion are directly dependent on surface type. Namely, glass stimulated adherent macrophages to produce the highest level of TNF-α secretion, with successively lower amounts detected for PU, CH-Q, and HA surfaces. The morphological results of cell size, contact area and degree

of spreading also generated a similar rank order, showing that both morphological and biofunctional measures can be used for biocompatibility evaluation.

Acknowledgments

This work was supported by the National Institutes of Health (NIH R01 HL60230). We thank Zhengzheng Liao and Ivan J. Dmochowski (Department of Chemistry at University of Pennsylvania) for confocal fluorescence microscopy. We also thank Benjamin J. Pichette (Department of Anesthesiology and Critical Care at University of Pennsylvania) and Michael J. A. Hore (Materials Science and Engineering at University of Pennsylvania) for data analysis. The Nano/Bio Interface Center at the University of Pennsylvania provided facility support for surface characterization (NSF/DMR08-32802).

References

1. Richards MJ, Edwards JR, Culver DH, Gaynes RP. Nosocomial infections in medical intensive care units in the United States. Crit Care Med. 1999; 27:887–892. [PubMed: 10362409]
2. Markowicz P, Wolff M, Djedaini K, Cohen Y, Chastre J, Delclaux C, Merrer J, Herman B, Veber B, Fontaine A, Dreyfuss D. Multicenter prospective study of ventilator-associated pneumonia during acute respiratory distress syndrome - Incidence, prognosis, and risk factors. Am J Resp Crit Care. 2000; 161:1942–1948.
3. Martin DC, O'Ryan FS, Indresano AT, Bogdanos P, Wang B, Hui RL, Lo JC. Characteristics of implant failures in patients with a history of oral bisphosphonate therapy. J Oral Maxil Surg. 2010; 68:508–514.
4. Baddour LM, Bettmann MA, Bolger AF, Epstein AE, Ferrieri P, Gerber MA, Gewitz MH, Jacobs AK, Levison ME, Newburger JW, Pallasch TJ, Wilson WR, Baltimore RS, Falace DA, Shulman ST, Tani LY, Taubert KA. Nonvalvular cardiovascular device-related infections. Circulation. 2003; 108:2015–2031. [PubMed: 14568887]
5. Bernacca GM, Mackay TG, Wilkinson R, Wheatley DJ. Calcification and fatigue failure in a polyurethane heart valve. Biomaterials. 1995; 16:279–285. [PubMed: 7772667]
6. Kirkpatrick CJ, Bittinger F, Wagner M, Kohler H, van Kooten TG, Klein CL, Otto M. Current trends in biocompatibility testing. P I Mech Eng H. 1998; 212:75–84.
7. Anderson JM. Biological responses to materials. Annu Rev Mater Res. 2001; 31:81–110.
8. Anderson JM, Rodriguez A, Chang DT. Foreign body reaction to biomaterials. Semin Immunol. 2008; 20:86–100. [PubMed: 18162407]
9. Xia Z, Triffitt JT. A review on macrophage responses to biomaterials. Biomed Mater. 2006; 1:R1–9. [PubMed: 18458376]
10. Luttikhuizen DT, Harmsen MC, Van Luyn MJA. Cellular and molecular dynamics in the foreign body reaction. Tissue Eng. 2006; 12:1955–1970. [PubMed: 16889525]
11. Takebe J, Champagne CM, Offenbacher S, Ishibashi K, Cooper LF. Titanium surface topography alters cell shape and modulates bone morphogenetic protein 2 expression in the J774A. 1 macrophage cell line. J Biomed Mater Res A. 2003; 64A:207–216. [PubMed: 12522806]
12. Lu J, Descamps M, Dejou J, Koubi G, Hardouin P, Lemaitre J, Proust JP. The biodegradation mechanism of calcium phosphate biomaterials in bone. J Biomed Mater Res. 2002; 63:408–412. [PubMed: 12115748]
13. Solheim E, Sudmann B, Bang G, Sudmann E. Biocompatibility and effect on osteogenesis of poly(ortho ester) compared to poly(DL-lactic acid). J Biomed Mater Res. 2000; 49:257–263. [PubMed: 10571914]
14. Labow RS, Sa D, Matheson LA, Santerre JP. Polycarbonate-urethane hard segment type influences esterase substrate specificity for human-macrophage-mediated biodegradation. J Biomat Sci-Polym E. 2005; 16:1167–1177.
15. Schutte RJ, Xie L, Klitzman B, Reichert WM. In vivo cytokine-associated responses to biomaterials. Biomaterials. 2009; 30:160–168. [PubMed: 18849070]
16. Khouw IMSL, van Wachem PB, de Leij LFMH, Van Luyn MJA. Inhibition of the tissue reaction to a biodegradable biomaterial by monoclonal antibodies to IFN-g. J Biomed Mater Res. 1998; 41:202–210. [PubMed: 9638524]

17. Tan KS, Qian L, Rosado R, Flood PM, Cooper LF. The role of titanium surface topography on J774A. 1 macrophage inflammatory cytokines and nitric oxide production. Biomaterials. 2006; 27:5170–5177. [PubMed: 16808973]

18. Paula NE, Skazik C, Harwardt M, Bartneck M, Denecke B, Klee D, Salber J, Zwadlo-Klarwasser G. Topographical control of human macrophages by a regularly micro structured polyvinylidene fluoride surface. Biomaterials. 2008; 29:4056–4064. [PubMed: 18667233]

19. Brodbeck WG, Nakayama Y, Matsuda T, Colton E, Ziats NP, Anderson JM. Biomaterial surface chemistry dictates adherent monocyte/macrophage cytokine expression in vitro. Cytokine. 2002; 18:311–319. [PubMed: 12160519]

20. Jones JA, Chang DT, Meyerson H, Colton E, Kwon IK, Matsuda T, Anderson JM. Proteomic analysis and quantification of cytokines and chemokines from biomaterial surface-adherent macrophages and foreign body giant cells. J Biomed Mater Res A. 2007; 83A:585–596. [PubMed: 17503526]

21. Jang JY, Lee DY, Park SJ, Byun Y. Immune reactions of lymphocytes and macrophages against PEG-grafted pancreatic islets. Biomaterials. 2004; 25:3663–3669. [PubMed: 15020141]

22. Refai AK, Textor M, Brunette DM, Waterfield JD. Effect of titanium surface topography on macrophage activation and secretion of proinflammatory cytokines and chemokines. J Biomed Mater Res A. 2004; 70A:194–205. [PubMed: 15227664]

23. Cardona MA, Simmons RL, Kaplan SS. TNF and Il-1 Generation by Human Monocytes in Response to Biomaterials. J Biomed Mater Res. 1992; 26:851–859. [PubMed: 1535076]

24. Tsai IY, Kuo CC, Tomczyk N, Stachelek SJ, Composto RJ, Eckmann DM. Human macrophage adhesion on polysaccharide patterned surfaces. Soft Matter. 2011; 7:3599–3606. [PubMed: 21479122]

25. Dinnes DLM, Santerre JP, Labow RS. Influence of biodegradable and non-biodegradable material surfaces on the differentiation of human monocyte-derived macrophages. Differentiation. 2008; 76:232–244. [PubMed: 17924965]

26. Brodbeck WG, Patel J, Voskerician G, Christenson E, Shive MS, Nakayama Y, Matsuda T, Ziats NP, Anderson JM. Biomaterial adherent macrophage apoptosis is increased by hydrophilic and anionic substrates in vivo. P Natl Acad Sci USA. 2002; 99:10287–10292.

27. Wan LS, Xu ZK, Huang XJ, Huang XD, Yao K. Cytocompatibility of poly(acrylonitrile-co-N-vinyl-2-pyrrolidone) membranes with human endothelial cells and macrophages. Acta Biomater. 2007; 3:183–190. [PubMed: 17150422]

28. Lin DT, Young TH, Fang Y. Studies on the effect of surface properties on the biocompatibility of polyurethane membranes. Biomaterials. 2001; 22:1521–1529. [PubMed: 11374451]

29. Christenson EM, Dadsetan M, Anderson JM, Hiltner A. Biostability and macrophage-mediated foreign body reaction of silicone-modified polyurethanes. J Biomed Mater Res A. 2005; 74A:141–155. [PubMed: 16201029]

30. Lee H, Eckmann DM, Lee D, Composto RJ. pH-Dependent swelling of grafted chitosan on surfaces. PMSE preprints. 2011; 104:41–42.

31. Lee H, Eckmann DM, Lee D, Hickok NJ, Composto RJ. Symmetric pH-dependent swelling and antibacterial properties of chitosan brushes. Langmuir. 2011; 27:12458–12465. [PubMed: 21894981]

32. Ombelli M, Costello L, Postle C, Anantharaman V, Meng QC, Composto RJ, Eckmann DM. Competitive protein adsorption on polysaccharide and hyaluronate modified surfaces. Biofouling. 2011; 27:505–518. [PubMed: 21623481]

33. Ferrer MCC, Yang S, Eckmann DM, Composto RJ. Creating biomimetic polymeric surfaces by photochemical attachment and patterning of dextran. Langmuir. 2010; 26:14126–14134. [PubMed: 20712352]

34. Tsai IY, Tomczyk N, Eckmann JI, Composto RJ, Eckmann DM. Human plasma protein adsorption onto dextranized surfaces: a two-dimensional electrophoresis and mass spectrometry study. Colloid Surface B. 2011; 84:241–252.

35. Li C, Han J, Huang Q, Xu H, Tao H, Li X. Microstructure development of thermoplastic polyurethanes under compression: The influence form first-order structure to aggregation structure and a structural optimization. Polymer. 2012; 53:1138–1147.

36. Endo M, Zoltick PW, Chung DC, Bennett J, Radu A, Muvarak N, Flake AW. Gene transfer to ocular stem cells by early gestational intraamniotic injection of lentiviral vector. Mol Ther. 2007; 15:579–587. [PubMed: 17245352]
37. Sena-Esteves M, Tebbets JC, Steffens S, Crombleholme T, Flake AW. Optimized large-scale production of high titer lentivirus vector pseudotypes. J Virol Methods. 2004; 122:131–139. [PubMed: 15542136]
38. Stachelek SJ, Finley MJ, Alferiev IS, Wang FX, Tsai RK, Eckells EC, Tomczyk N, Connolly JM, Discher DE, Eckmann DM, Levy RJ. The effect of CD47 modified polymer surfaces on inflammatory cell attachment and activation. Biomaterials. 2011; 32:4317–4326. [PubMed: 21429575]
39. Laemmli UK. Cleavage of Structural Proteins during the Assembly of the Head of Bacteriophage T4. Nature. 1970; 227:680–685. [PubMed: 5432063]
40. Stachelek SJ, Alferiev I, Fulmer J, Ischiropouios H, Levy RJ. Biological stability of polyurethane modified with covalent attachment of di-tert-butyl-phenol. J Biomed Mater Res A. 2007; 82A: 1004–1011. [PubMed: 17370325]
41. Chang CC, Lieberman SM, Moghe PV. Leukocyte spreading behavior on vascular biomaterial surfaces: consequences of chemoattractant stimulation. Biomaterials. 1999; 20:273–281. [PubMed: 10030604]
42. Schubert MA, Wiggins MJ, Anderson JM, Hiltner A. Comparison of two antioxidants for poly(etherurethane urea) in an accelerated in vitro biodegradation system. J Biomed Mater Res. 1997; 34:493–505. [PubMed: 9054533]
43. Daigneault M, Preston JA, Marriott HM, Whyte MKB, Dockrell DH. The Identification of markers of macrophage differentiation in PMA-stimulated THP-1 cells and monocyte-derived macrophages. PLoS One. 2010; 5:e8668. [PubMed: 20084270]
44. Murao S, Gemmell MA, Callaham MF, Anderson NL, Huberman E. Control of macrophage cell-differentiation in human promyelocytic Hl-60 leukemia-cells by 1,25-dihydroxyvitamin-D3 and phorbol-12-myristate-13-acetate. Cancer Res. 1983; 43:4989–4996. [PubMed: 6576856]
45. Park EK, Jung HS, Yang HI, Yoo MC, Kim C, Kim KS. Optimized THP-1 differentiation is required for the detection of responses to weak stimuli. Inflamm Res. 2007; 56:45–50. [PubMed: 17334670]
46. Brodbeck WG, Shive MS, Colton E, Nakayama Y, Matsuda T, Anderson J. Influence of biomaterial surface chemistry on the apoptosis of adherent cells. J Biomed Mater Res. 2001; 55:661–668. [PubMed: 11288096]
47. Amato PA, Unanue ER, Taylor DL. Distribution of actin in spreading macrophages - a comparative-study on living and fixed Cells. J Cell Biol. 1983; 96:750–761. [PubMed: 6339523]
48. Stendahl OI, Hartwig JH, Brotschi EA, Stossel TP. Distribution of actin-binding protein and myosin in macrophages during spreading and phagocytosis. J Cell Biol. 1980; 84:215–224. [PubMed: 6991506]
49. Baba T, Shiozawa N, Hotchi M, Ohno S. Three-dimensional study of the cytoskeleton in macrophages and multinucleate giant cells by quick-freezing and deep-etching method. Virchows Arch. 1992; 61:39–47.
50. Tsai RK, Discher DE. Inhibition of “self” engulfment through deactivation of myosin-II at the phagocytic synapse between human cells. J Cell Biol. 2008; 180:989–1003. [PubMed: 18332220]

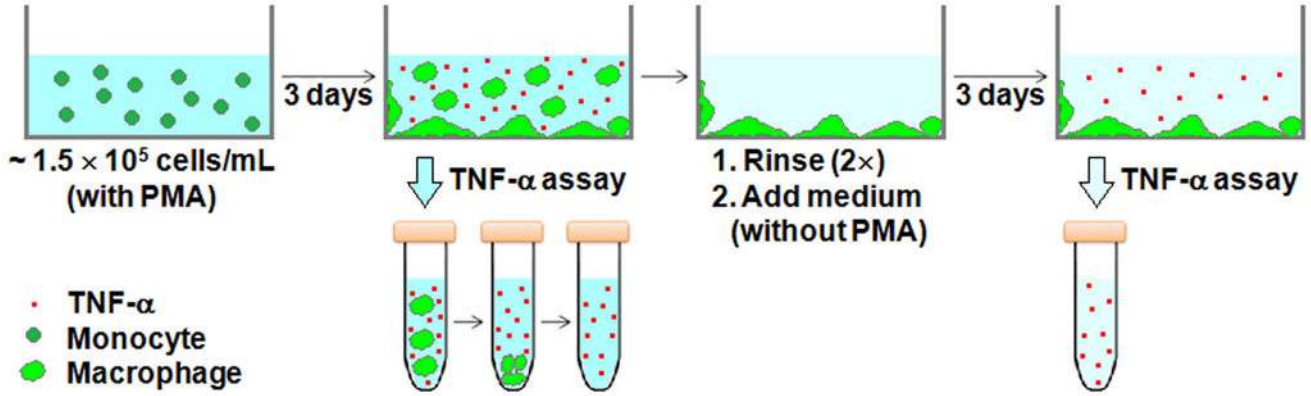

FIGURE 1.
Experimental scheme for measurement of TNF-α secretion by adherent macrophages (PMA-differentiated THP-1) on surfaces of glass, polyurethane (PU), chitosan possessing quaternary ammonium salts (CH-Q) and hyaluronic acid (HA). The cell culture medium volume is 7 mL for these experiments.

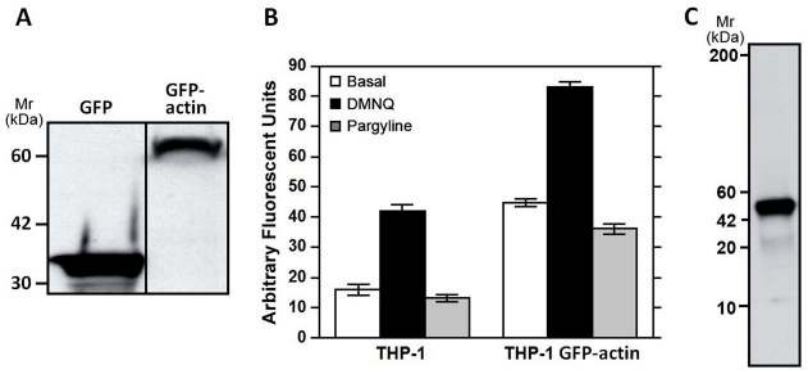

FIGURE 2.

(A) THP-1 was transduced with the GFP-actin gene via a lentiviral vector (THP-1 GFP-actin). Western blot analysis of GFP expression from THP-GA lysates expressing GFP control or GFP-actin confirms the presence of the chimeric protein. (B) Cultured THP-1 cells (10^5) or THP-1 GFP-actin cells were seeded on PE films inserted on the bottom of 96 well plates. After 2 hr the culture medium was replaced with DHR-123 containing medium and cells were incubated for 2 hr at 37°C. Cells were rinsed twice with PBS, and 10^{-5} M of pargyline, a monoamine oxidase antagonist, or a superoxide initiator DMNQ was added to triplicate wells. Fluorescence (500 nm excitation, 536 nm emission) was measured at one hr. Higher values in the transduced cells are due to GFP expression. Results show identical trends in ROS production irrespective of GFP-actin treatment, thus strongly suggesting that the GFP-actin expression had no untoward effect upon normal MDM function. Data are presented as mean ± SD (n = 4 experiments). (C) Representative Western blot analysis of THP-1 GFP-actin expressing cell lysates immunoprecipitated with GFP-actin antibody and probed for the expression of the actin-binding protein Fascin.

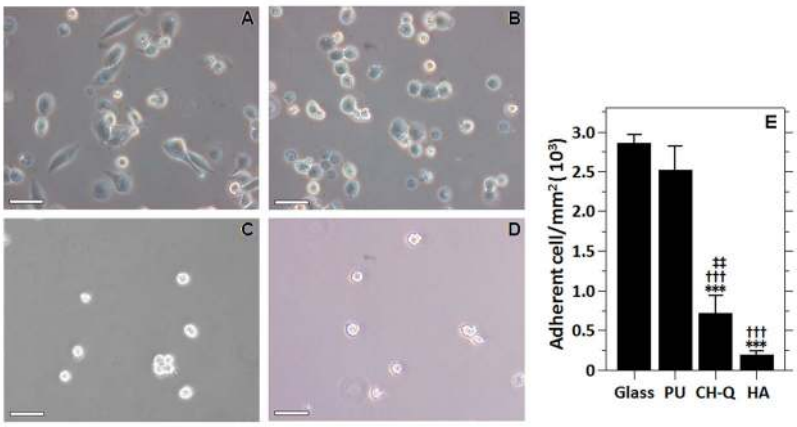

FIGURE 3.

Morphology of monocyte-derivatized macrophages (PMA-treated THP-1 cells) on (A) glass, (B) PU, (C) CH-Q, and (D) HA after three days. (A) Macrophages on the glass show amoeboid morphology, similar to macrophages adherent to polystyrene culture dishes. (B) Macrophages on PU demonstrate a round morphology. (C) Macrophages on CH-Q show a round morphology, a low cell surface density and small size, similar to cells attached to HA as shown in (D). Scale bar length is 50 μm. (E) Adhesion density of macrophages on the four surface types after three days. Data are presented as mean ∓standard deviation (n = 3 experiments). Statistical significance: ***$P < 0.001$ versus glass, $^{\dagger\dagger\dagger}P < 0.001$ versus PU, $^{\ddagger\ddagger}P < 0.01$ versus HA, $^{\ddagger\ddagger\ddagger}P < 0.001$ versus HA.

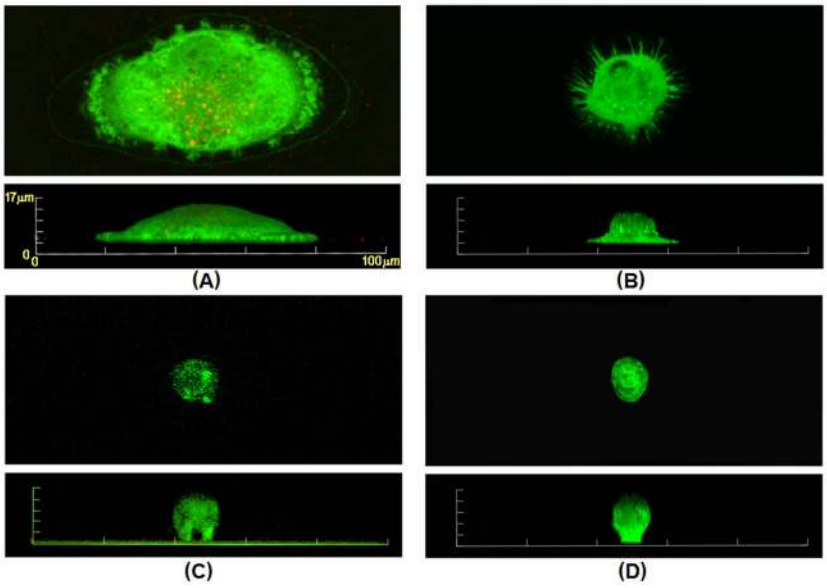

FIGURE 4.

Representative 3-D confocal fluorescence images of monocyte-derived macrophages (PMA-treated GFP-actin transduced THP-1 cells) on (A) glass, (B) PU, (C) CH-Q and (D) HA surfaces after three days of culturing. The images represent maximal cell projection along the optical axis (z-axis, top view in each panel A–D) and a side projection (y-axis, side view in each panel A–D). The identical y and z scales shown in (A) were used for all images.

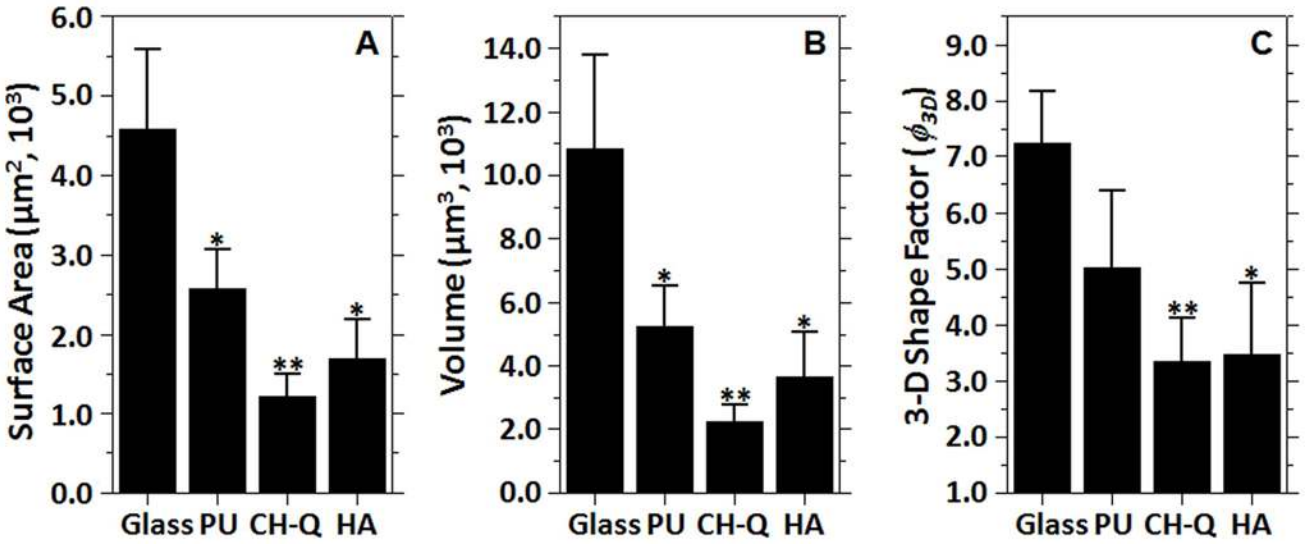

FIGURE 5.

(A) Cell surface area and (B) cell volume for macrophages adherent to glass, PU, CH-Q and HA surfaces. (C) Degree of cell spreading for macrophages adherent to the four surface types. The calculated 3-D shape factor $\varphi_{3D} = 1$ for a perfectly spherical object. Data are presented as mean ±standard deviation (n = 3 experiments). Statistical significance: *P < 0.05 versus glass, **P < 0.01 versus glass.

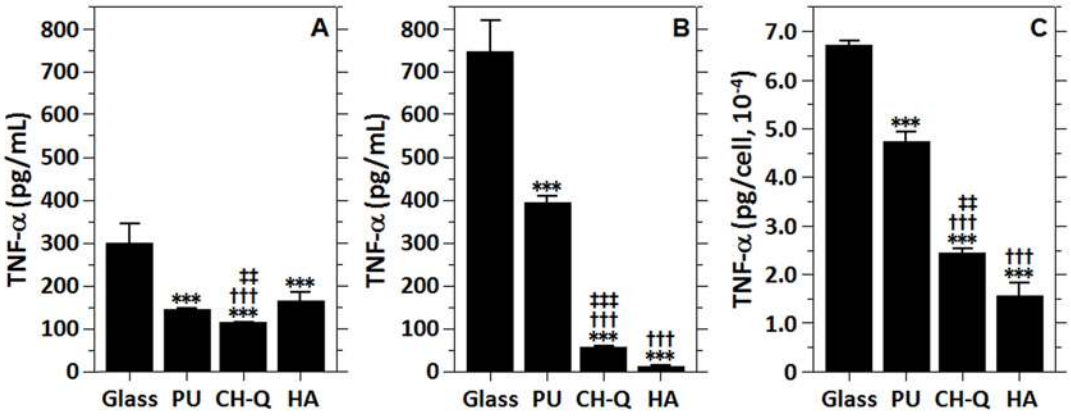

FIGURE 6.

(A) ELISA assay results of TNF-αlevels secreted by suspended and adherent macrophages cultured in glass dishes and PU-coated, CH-Q coated, HA coated glass dishes for three days. (B) TNF-αsecretion from adherent macrophages cultured for three additional days in each dish after rinsing and replacing the medium to remove suspended cells. (C) Normalized TNF-αsecretion levels per adherent cell on each surface type. Data are presented as mean ±standard deviation (n = 3 experiments). Statistical significance: ***P < 0.001 versus glass, †††P < 0.001 versus PU, ‡‡P < 0.01 versus HA, ‡‡‡P < 0.001 versus HA.